



Poly(azomethine-epoxy-ether) containing phenyl and etoxy moieties: synthesis, characterization and fluorescence property

Feyza Kolcu^{1,2} · İsmet Kaya¹

Received: 20 February 2018 / Accepted: 30 May 2018
© Institute of Chemistry, Slovak Academy of Sciences 2018

Abstract

The design and synthesis of poly(azomethine-epoxy-ether) (PAZ-EP) containing epoxide moiety was described. The purpose of the research was the improvement of poly(azomethine-ether) containing epoxide by introduction of Schiff base moiety. PAZ-EP was synthesized using epichlorohydrin (EP). The structure of the Schiff base (SB) and PAZ-EP were verified by FT-IR, ¹H-NMR, ¹³C-NMR and UV–Vis spectroscopic analyses. Further characterization was employed using photophysical, electrochemical and fluorescence (PL) measurements. Application of TGA and differential scanning calorimetry analyses revealed thermal stability and thus propose a thermal processibility, which makes them potential materials for many contemporary practices. The number of average molecular weight of polymer with a polydispersity index of 1.14 was found to be 6750 Da using a gel permeation chromatography instrument. The highest occupied–lowest unoccupied energy levels and electrochemical (E_g^r) band gap values of PAZ-EP were determined by cyclic voltammetry (CV) measurement. Scanning electron microscopy (SEM) images were illustrated at different magnifications to study the morphologic property of PAZ-EP.

Keywords Poly(azomethine-ether) · Epichlorohydrin · SEM · Photoluminescence

Introduction

Poly(azomethine) (PAM) containing imine group (C=N) in the backbone are a potential category of polymers owing to their high mechanical strength, thermal stability, metal-chelating ability, liquid crystalline potential and semiconducting electrical properties under doping (Kobzar et al. 2016; Pron and Rannou 2002; Grigoras and Catanescu 2004; Iwan and Sek 2008; Kumar et al. 2009; Hussein et al. 2012; Zhang et al. 2014; Ravikumar et al. 2014). PAMs are crucial conjugated polymers attracting the researchers' interest for their applications in optoelectronics, electronics, sensors

and photonics wherefore their good mechanical properties, thermal stability and molecular-doping-controlled features (Iwan and Sek 2008; Sek et al. 2008; Barik and Skene 2011; Bourgeaux and Skene 2007; Niu et al. 2011; Park et al. 2010; Işık et al. 2012; Ma et al. 2015; Koole et al. 2016, Marin et al. 2017; Yeh et al. 2016).

The synthesis of poly(azomethine)s (PAM)s is achieved under the traditional path using a polycondensation of diamine and dialdehyde (Iwan and Sek 2008; Saegusa et al. 1994; Gutch et al. 2001; Grimm et al. 2002; Choi et al. 2004; Fukukawa et al. 2004; Krebs and Jørgensen 2004; Ishii et al. 2010; Cerrada et al. 1996). The macromolecular chains of PAMs with high molecular weight precipitated from the solution have slight solubility in common organic solvents, which is considered as a major drawback in their practical applications (Grigoras and Catanescu 2004; Iwan and Sek 2008; Hussein et al. 2012; Stefanache et al. 2014). Due to the aforementioned problem, poly(azomethine-ether)s, poly(azomethine-urethane)s and poly(azomethine-ester)s included in PAMs have been lately synthesized using several techniques (Dutta et al. 2003; Shukla et al. 2003). The participation of aliphatic units and flexible ether linkages along the polymer chain provides fractional mobility to the

✉ Feyza Kolcu
feyzakolcu@comu.edu.tr

✉ İsmet Kaya
kayaismet@hotmail.com

¹ Department of Chemistry, Polymer Synthesis and Analysis Laboratory, Çanakkale Onsekiz Mart University, 17020 Çanakkale, Turkey

² Department of Chemistry and Chemical Processing Technologies, Lapseki Vocational School, Çanakkale Onsekiz Mart University, Çanakkale, Turkey

polymers and consequently, intensifies their solubility (Gul et al. 2014; Marin et al. 2006). The incorporation of the flexible aliphatic segments into poly(azomethine) chains is indeed a method to induce the occurrence of the liquid crystalline properties (Grigoras and Catanescu 2004; Hussein et al. 2012; Abid and Al-barody 2014). The azomethine linkage can be easily obtained in mild reaction conditions (Nitschke et al. 2017; Kaya et al. 2018).

Epoxy resins are reactive intermediates used to produce a versatile class of thermosetting polymers. They are characterized by the presence of a three-member cyclic ether group commonly referred to as an epoxy group, or oxirane. The largest single use of epoxy resins is in the protective coatings market where high corrosion resistance and adhesion to substrates are important. Epoxies gain wide acceptance in protective coatings and in electrical and structural applications because of their exceptional combination of properties such as toughness, adhesion, chemical and thermal resistance, and good electrical properties (Adams and Gannon 1986).

From application point of view, the aim of this study was to design a poly(azomethine) by a chemical structure modification (introduction of solubility epoxy group as a side chain) and to see the impacts on the optical, thermal, morphological and fluorescence properties. The synthesis of poly(azomethine-epoxy-ether) (PAZ-EP) was divided into three steps: (1) synthesis of dialdehyde, (2) synthesis of Schiff base containing diol, and (3) synthesis of poly(azomethine-ether) (PAZ-EP). FT-IR, ^1H NMR and ^{13}C NMR analyses were performed for the structural characterization of the products obtained in each step. Thermal stability and the transition temperatures were analyzed using thermogravimetric techniques (TG) and differential scanning calorimetry (DSC), respectively. Optical, photoluminescence (PL) and electrochemical properties were investigated using UV-Vis, fluorescence spectroscopy and cyclic voltammetry (CV), respectively.

Experimental

Materials

4-({4-[(4-Formylphenoxy)methyl]benzyl}oxy)benzaldehyde, abbreviated as (DA) was synthesized based on the previously reported procedure (Kaya and Culhaoglu 2009). 4-Hydroxybenzaldehyde (4-HB), 4-aminophenol (4-AP), *p*-xylene dibromide (XB), diglycolamine agent (DGA, 98%) and epichlorohydrin (EP, 99%) purchased from Sigma-Aldrich Chemical Company (Germany) were used as received. Methanol, ethanol, chloroform, *N,N*-dimethylformamide (DMF), tetrahydrofuran (THF), dimethyl sulfoxide (DMSO), toluene, acetonitrile, and all other solvents used

were provided by Merck Chemical Company (Germany), and used with no further purification.

Synthesis of dialdehyde (DA)

The synthetic procedure for dialdehyde monomer, (DA) was presented according to the literature (Kaya and Culhaoglu 2009) in Scheme 1. 4-Hydroxybenzaldehyde, 0.740 g, 0.006 mol) in 30 mL of DMF was placed into 250 mL three-necked flask provided with a condenser and magnetic stirrer, and containing anhydrous sodium carbonate (0.795 g, 0.0075 mol). *p*-Xylene dibromide (0.792 g, 0.003 mol) dissolved in 30 mL of DMF was added into the reaction mixture under argon atmosphere. The mixture was maintained for 4 h at 150 °C. As soon as it cooled, the product was transferred into 200 mL of cold water. After completing the washing process of the precipitated dialdehyde with 200 mL of water, it was filtered to separate mineral salts. The product of DA was recrystallized from methanol and dried in a vacuum oven for a day at 50 °C.

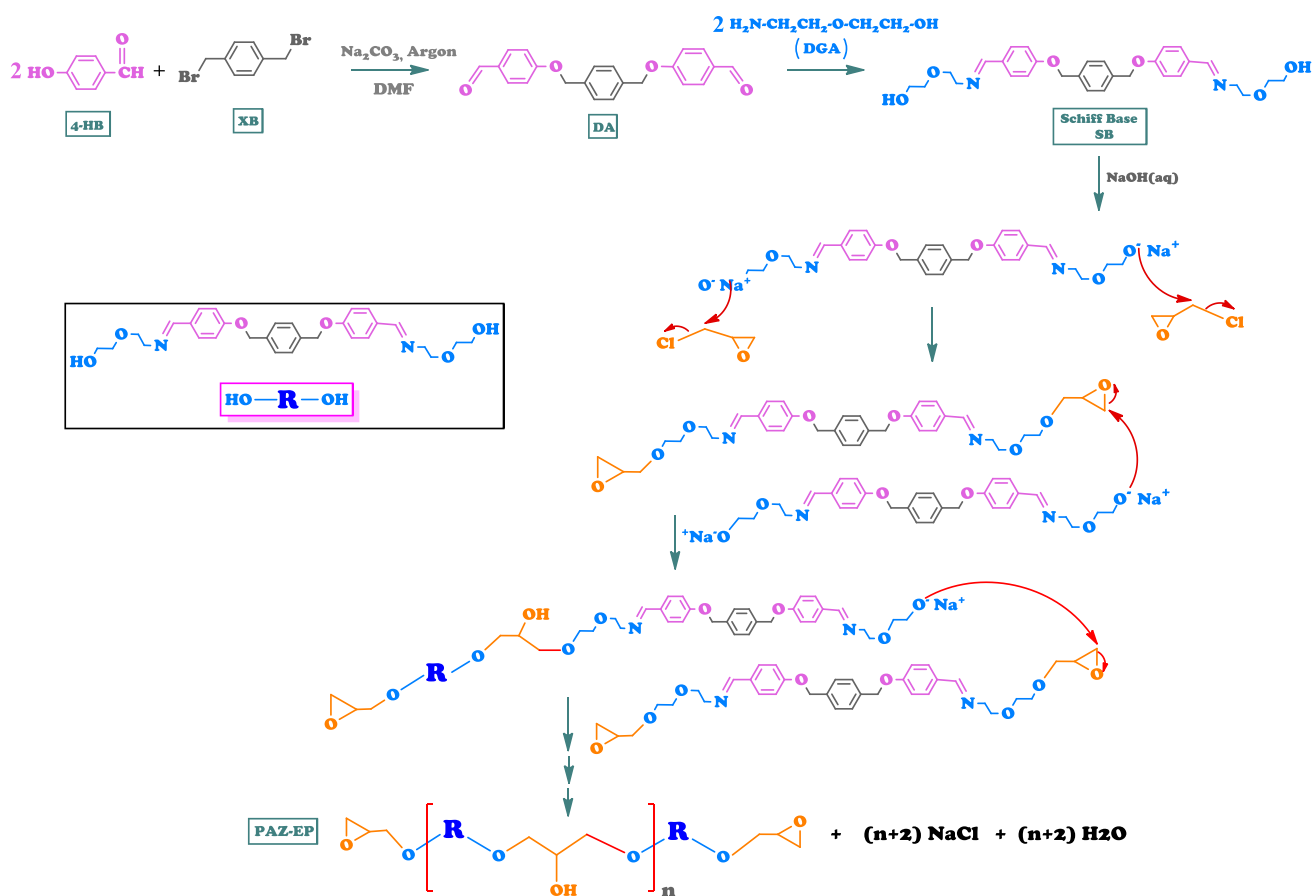
For DA Yield 45%; melting point: 166–167 °C; Elemental analyses results: Calc. (Found): C, 76.28 (76.20); H, 5.23 (5.19). ^1H NMR (DMSO- d_6 , δ_{H} ppm): 9.88 (s, 2H, $-\text{CHO}$), 7.87–7.49 (m, 12H, aromatic hydrogens), 5.18 ppm (s, 4H, aliphatic hydrogens); ^{13}C NMR (DMSO- d_6 , δ ppm): 190.69 (aldehyde $-\text{CHO}$), 163.47–115.29 (aromatic $-\text{CH}$), 70.70 ppm (aliphatic $-\text{CH}$).

Synthesis of Schiff base

To synthesize Schiff base (SB), a mixture of DGA (0.314 g, 0.003 mol) and DA (0.519 g, 0.0015 mol) dissolved in 25 mL DMF were placed in a 250 mL three-necked round bottom-flask provided with a reflux condenser and a collector tube. Reaction mixture was refluxed for 6 h at 105 °C under argon atmosphere. As soon as it cooled to room temperature, the Schiff base was precipitated, filtered off, washed by methanol (3 \times 50 mL) and dried at 50 °C for a day in a vacuum oven. The synthesis of Schiff base was presented in Scheme 1. The yield was found to be 70%.

Elemental analyses results: Calc. (Found): C, 69.23 (69.05); H, 6.92 (6.85); N, 5.39 (5.32).

For SB FT-IR (cm^{-1}): 3334 ν ($-\text{OH}$), 2922 ν (C–H, aromatic), 2840 ν (C–H, aliphatic), 1678 ν (C=O, impurity), 1642 ν (C=N), 1598, 1505 ν (C=C phenyl), 1350 ν (C–N), 1244 ν (C–O, phenyl). ^1H NMR (DMSO- d_6): δ_{H} ppm, 8.23 (s, 2H, $-\text{CH}=\text{N}-$), 7.75 (d, $J=98$ Hz, 4H, He), 7.46 (s, 4H, Hh), 7.12 (d, $J=78$ Hz, 4H, Hf), 5.17 (t, $J=24$ Hz, 4H, Hd), 4.57 (s, 4H, Hg), 3.64 (s, 2H, $-\text{OH}$), 3.46 (t, $J=24$ Hz, 4H, Hc), 3.42 (t, $J=15$ Hz, 4H, Hb), 3.36 (t, $J=15$ Hz, 4H, Ha). ^{13}C NMR (DMSO- d_6): δ ppm, 163.64 (C8), 161.63 (C4), 136.91 (C2), 132.23 (C7), 129.90 (C6), 128.37 (C1),



Scheme 1 Possible mechanism for the synthesis of dialdehyde (DA), Schiff base (SB) and poly(azomethine-epoxy-ether) (PAZ-EP)

115.71 (C5), 72.65 (C10), 70.70 (C3), 69.81 (C11), 69.51 (C9), 60.66 (C12).

Synthesis of poly(azomethine-epoxy-ether) (PAZ-EP)

The synthesis of PAZ-EP is outlined in Scheme 1 and the synthetic procedure of a different type of PAZ-EP was given in a previous study (Kaya et al. 2011). The epoxidation of the synthesized Schiff base was carried out by refluxing SB and EP in 1:2 mol ratio placed in a three-necked round-bottom flask equipped with a condenser, thermometer and dropping funnel. The reaction mixture was maintained at 40 °C under nitrogen atmosphere for 1 h followed by raising the reaction temperature up to 90 °C. A concentrated solution of 50% NaOH (2 mL) transferred to a dropping funnel was added to the reaction mixture in 2 h by stirring. The solid product obtained from a rotary evaporator was dissolved in THF. The salt was removed by filtering the solution. The excess EP and THF were separated by distillation under reduced pressure. The yield of PAZ-EP was found to be 79%. The synthesis of Schiff base is outlined in Scheme 1.

Elemental analyses results: Calc. (Found): C, 68.75 (68.25); H, 6.94 (6.50); N, 4.86 (4.35).

For PAZ-EP FT-IR (cm^{-1}): 3334 $\nu(\text{OH})$, 2944 $\nu(\text{C-H, aromatic})$, 2876 $\nu(\text{C-H, aliphatic})$, 1648 $\nu(\text{C=N})$, 1601, 1510 $\nu(\text{C=C phenyl})$, 1360 $\nu(\text{C-N})$, 1241 $\nu(\text{C-O, phenyl})$. $^1\text{H NMR}$ (DMSO-d_6): δ_{H} ppm, 8.25 (s, $-\text{CH}=\text{N}$), 7.85 (d, $J=12$ Hz, He), 7.47 (s, Hh), 7.17 (d, $J=12$ Hz, Hf), 5.21 (t, $J=6$ Hz, Hd), 5.12 (s, Hg), 4.74 (d, $J=54$ Hz, Hk), 4.44 (d, $J=36$ Hz, Hm), 3.89 (t, $J=6.0$ Hz, Hl), 3.77 (s, 2H, $-\text{OH}$), 3.61 (t, $J=6$ Hz, Hc), 3.32 (t, $J=12$ Hz, Ha), 3.42 (t, $J=12$ Hz, Hb). $^{13}\text{C NMR}$ (DMSO-d_6): δ ppm, 163.64 (C8), 162.90 (C4), 136.62 (C2), 132.24 (C7), 130.22 (C6), 128.42 (C1), 115.73 (C5), 78.78 (C18), 78.62 (C15), 72.91 (C10), 71.69 (C3), 70.92 (C11), 70.30 (C9), 69.80 (C12), 63.46 (C14, C17), 63.06 (C16), 62.70 (C13).

Characterization

To carry out the solubility test in various solvents at room temperature, 1 mg of sample and 1 mL of solvent were used. Fourier transform infrared (FT-IR) spectrometry (Perkin Elmer FT-IR with ATR sampling accessory between wave numbers of 650 and 4000 cm^{-1} , USA) was employed to

identify the functional groups on the polymer. All samples were dissolved in dimethyl sulfoxide- d_6 to obtain ^1H and ^{13}C -NMR spectra using Agilent Premium compact FT-NMR series performing at the range of 600 and 150 MHz, respectively. As an internal standard, tetramethylsilane was used in NMR measurements. Elemental analyses of the compounds were carried out by a CHNS (Costech ECS 4010) analyzer. Gel permeation chromatography–light scattering (GPC–LS) instrument of Malvern Viscotek GPC Dual 270 max (UK) was employed to perform for the measurements of the polydispersity index (PDI), the number-average molecular weight (M_n), the average molecular weight (M_w), the viscosity average molecular weight (M_v) and the Z-average molecular weight (M_z) with a light-scattering detector (LS) of a medium 8.00 mm \times 300 mm Dual column and a refractive index detector (RID). DMF at a flow rate of 1 mL min^{-1} was used as eluent including 40 mM LiBr. GPC analysis was carried out at a column temperature of 55 °C. The calibration of the instrument was completed using a mixture of polystyrene standards (Polymer Laboratories; the peak molecular weights, M_p , between 162 and 60,000).

Ultraviolet–visible (UV–Vis) spectra were recorded to investigate the optical properties of the synthesized compounds in DMSO using Analytikjena Specord 210 Plus (United Kingdom) at room temperature. To obtain photoluminescence properties of the sample in DMSO, a Shimadzu RF-5301PC spectrofluorophotometer (Japan) was employed. Slit width in PL measurements was specified as 5 nm.

Thermogravimetric and differential thermal analyses (TG-DTG-DTA) using Perkin Elmer Pyris Sapphire (USA) were implemented to determine the mass change regarding thermal degradation for the polymer under nitrogen flow of 200 mL min^{-1} from ambient temperature up to 1000 °C at a heating rate of 10 °C min^{-1} . Differential scanning calorimetry (DSC, Perkin Elmer Sapphire) was used to determine the glass transition temperature (T_g) of the synthesized compounds between 25 and 420 °C under nitrogen atmosphere on the first heating run of 10 °C min^{-1} .

To investigate electrochemical properties, cyclic voltammetry (CV) assessments were performed using a CHI 660C Electrochemical Analyzer (Texas, USA) at a potential scan rate of 25 mV s^{-1} in a dry box filled with argon atmosphere at room temperature. Silver wire, glassy carbon electrode (GCE; $d=0.3$ cm in diameter) and platinum wire were used as a reference electrode, as a working electrode and as a counter electrode, respectively. The calibration of electrochemical potential of Ag was regulated with respect to the ferrocene/ferrocenium (Fc/Fc $^+$) couple. The half-wave potentials ($E^{1/2}$) of (Fc/Fc $^+$) in 0.1 M tetrabutylammonium hexafluorophosphate (TBAPF $_6$)/acetonitrile solution are 0.39 and 0.38 V vs. Ag wire and supporting calomel electrolyte, respectively. The voltammetric measurements were carried out in DMSO/acetonitrile mixture. The

electrochemical HOMO and LUMO energy levels and band gaps (E'_g) were estimated from the oxidation and reduction values (Cervini et al. 1997).

PAZ-EP was sprayed on an aluminum surface using a custom-built electro spinning setup, which consisted of a 2.5 mL syringe containing the polymer solution. The polymer solution was driven out of the syringe using an NE-300 single syringe pump (Pump Systems Inc., USA). A metal 25-gauge syringe needle (Cole Palmer Ltd., UK) was attached to the syringe. The needle tip and collecting plate were connected to a high voltage–power supply (model 73030P, Genvolt Ltd., UK). The applied voltage was set at 7 kV and flow rate of 1 mL h^{-1} was used. Distance between the needle tip and collecting plate was maintained at 12.5 cm.

Particle morphology was investigated using JEOL JSM 7100F field emission scanning electron microscopy (FE-SEM). Sputter coating process was used to create a thin gold/palladium film onto the polymer samples.

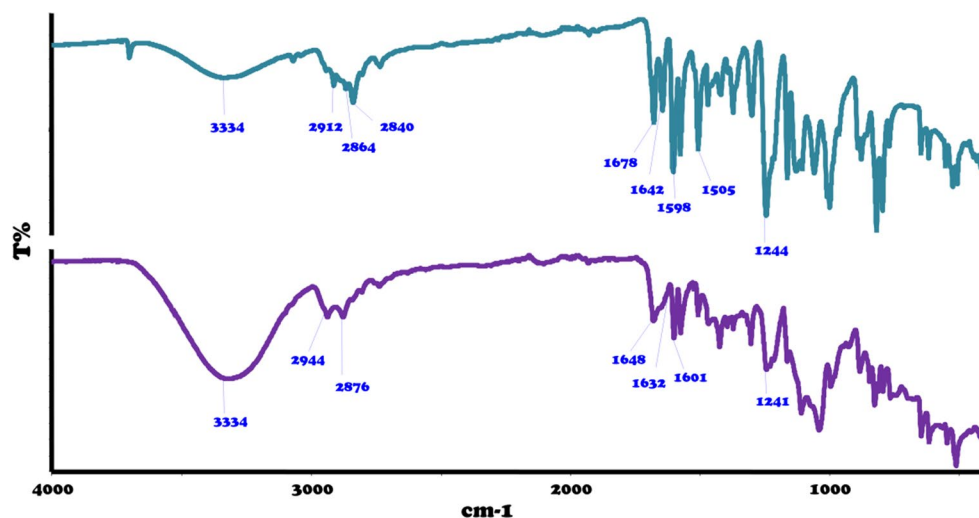
Results and discussion

Synthesis and characterization of SB and PAZ-EP

The synthesized Schiff base was in the form of yellow powder, whereas the polymerization of Schiff base resulted in highly viscous yellow colored PAZ-EP, as shown in Scheme 1. SB was soluble in aprotic polar solvents, DMSO and DMF in spite of partial solubility in polar solvents, such as ethanol. SB was insoluble in THF and acetonitrile. Epoxidation yielded an imine polymer PAZ-EP that was soluble in DMF, DMSO and ethanol, but insoluble in THF. Both SB and PAZ-EP were insoluble in methanol. In solvent with the reduced polarity, such as dichloromethane, hexane and heptane, SB and its imine polymer became insoluble.

The proposed mechanism for the syntheses of SB and PAZ-EP are given in Scheme 1. In NaOH solution, the sodium salt attacks the ethylene oxide, resulting in the ring opening reaction of epoxide. A water molecule comes along and the negative oxygen swipes a proton from it. This way, an –OH group appears and NaOH is regenerated. Oxirane rings are always present as terminal groups.

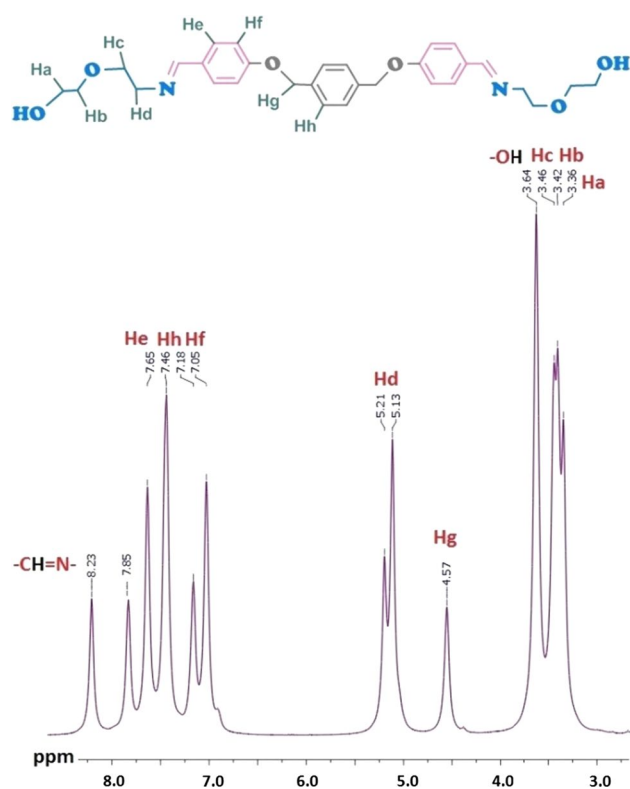
FT-IR spectra of the synthesized Schiff base and its imine polymer (PAZ-EP) are illustrated in Fig. 1. It is seen that the characteristic stretching vibrations of imine bond (C=N) were observed at 1642 and 1648 cm^{-1} for SB and PAZ-EP, respectively, proving the creation of azomethine linkage. The vibration at 1678 cm^{-1} of SB was attributed to C=O stretching frequency of DA as impurity which was removed by washing Schiff base by methanol. The peak at 3364 cm^{-1} was assigned to the O–H stretching mode of

Fig. 1 FT-IR spectra of SB and PAZ-EP

SB. The stretching frequency for O–H bond was seen as a broader peak around 3300 cm^{-1} in the spectrum of PAZ-EP due to the ring opening reaction of epoxide, as seen in Scheme 1. The absorption peaks at 2912 and 2944 cm^{-1} were attributable to the stretching modes of aromatic C–H bonds present in SB and PAZ-EP, respectively. The aliphatic C–H stretching modes were prominently observed at 2864 – 2840 cm^{-1} for SB, shifted to 2944 – 2876 cm^{-1} for PAZ-EP. In FT-IR spectra SB and PAZ-EP, the frequencies at 1244 and 1241 cm^{-1} were due to C–O–C vibrations.

To identify the structures, ^1H NMR spectra of SB and PAZ-EP are presented in Figs. 2 and 3, respectively. The resonance signals attributed to two imine ($-\text{CH}=\text{N}-$) and two primary $-\text{OH}$ protons were observed at 8.23 and 3.64 ppm, respectively, as seen in Fig. 2. The signal ratio of 14 protons in the range of 3.64 – 3.36 ppm, regarding to Ha, Hb, Hc and $-\text{OH}$, to $-\text{CH}=\text{N}-$ protons was found to be $14/2$. Additionally, the signal ratio of $-\text{CH}=\text{N}-$ to $-\text{OH}$ was found to be $2/2$, proving the formation of Schiff base. After epoxidation, ^1H NMR spectrum of PAZ-EP elucidated that $-\text{CH}=\text{N}-$ protons shifted downfield and were seen at 8.25 ppm (Fig. 3). The aromatic proton signals of He, Hf and Hh were observed in the range of 7.75 , 7.12 and 7.46 ppm and 7.85 , 7.17 and 7.47 ppm for SB and PAZ-EP, respectively. The multiplet peaks ranging from 3.61 to 3.28 ppm were interpreted as owing to the presence of aliphatic C–H protons of Ha, Hb and Hc in Fig. 3. The signal ratio of $-\text{CH}=\text{N}-$ protons to $-\text{OH}$ proton was found to be $2/1$, indicating that two azomethine protons were present together with one $-\text{OH}$ group in the unit structure of PAZ-EP. New peaks corresponding to a linkage of epichlorohydrin to SB appeared in the region of 4.74 – 3.89 ppm related to Hk, Hl and Hm protons of epichlorohydrin.

Evidently, the existence of carbon signal for azomethine at 163.64 ppm in Fig. 4 could be ascribed to the formation of Schiff base. The same carbon signal was also observed

**Fig. 2** ^1H NMR spectrum of SB

at 163.64 ppm in PAZ-EP. The only difference of PAZ-EP in carbon signals from SB was due to the presence of ethylene oxide and oxirane rings, as seen in Fig. 5. The carbon signals attributed to the ring opening reaction of epoxide were observed at 78.62 , 63.46 and 62.70 ppm for C15, C14 and C13, respectively. These results adequately indicated the establishment of a linkage between SB and EP. Three more carbon signals appeared at 78.78 , 63.46

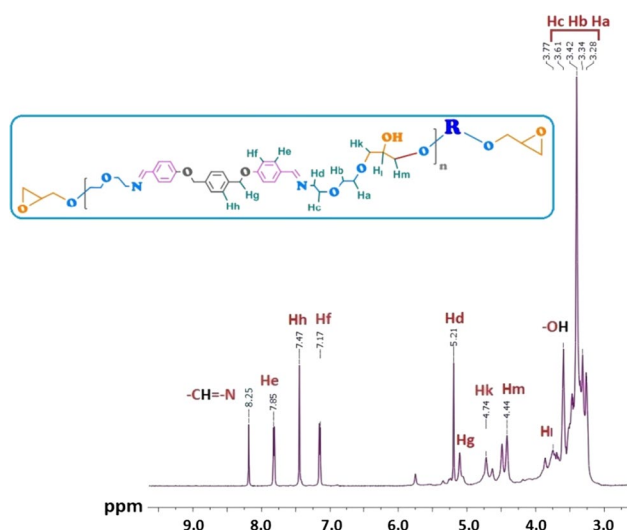


Fig. 3 ^1H NMR spectrum of PAZ-EP

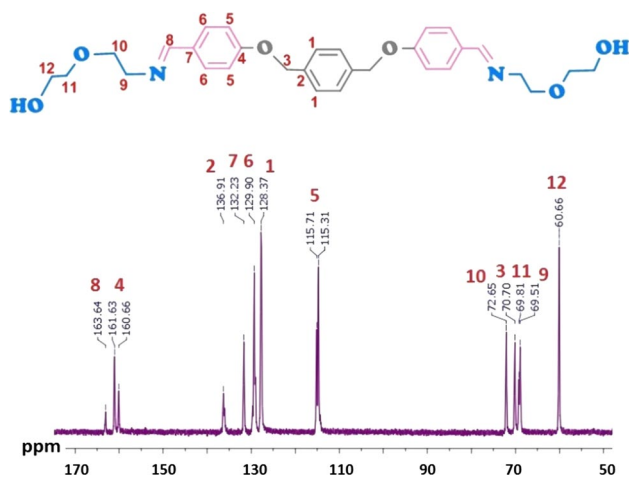


Fig. 4 ^{13}C NMR spectrum of SB

and 63.06 ppm for C18, C17 and C16, respectively, attributed to the ethylene oxide present as terminal groups.

GPC chromatogram indicated that M_n , M_w , M_v and M_z of PAZ-EP were calculated as 5900, 6750, 6800 and 5000 Da, respectively, with a mono modal particle size distribution. PAZ-EP had a polydispersity index (PDI) value of 1.14. The number for the constitutional units in PAZ-EP was found to be 10 and 12 with respect to the number-average molecular weight and the average molecular weight, respectively.

Photophysical and electrochemical properties

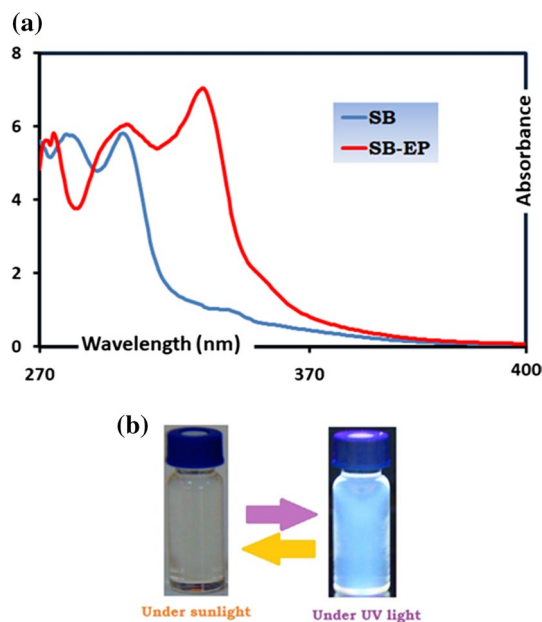
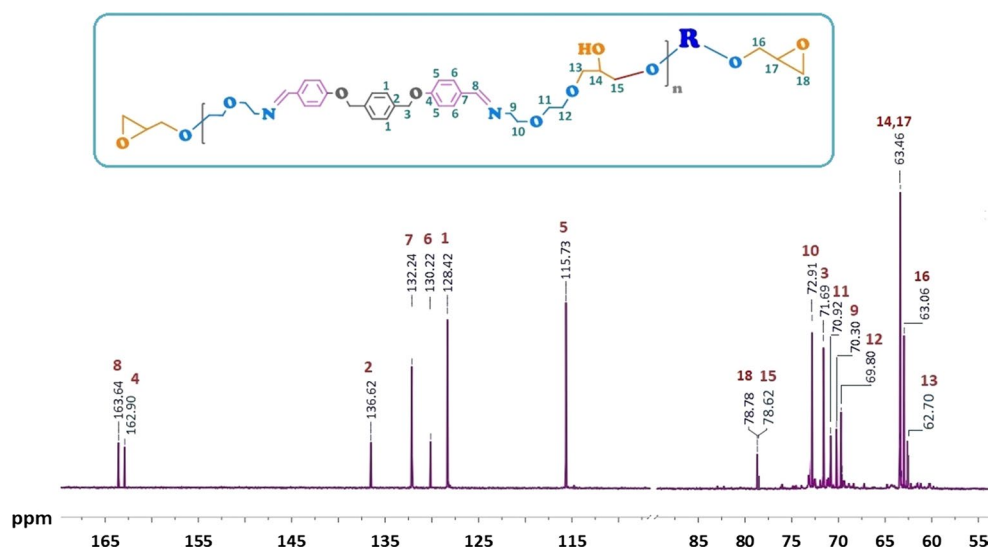
To have an insight into the electronic structure, photophysical properties of SB and PAZ-EP were analyzed using UV–Vis and photoluminescence spectroscopy in DMF

solutions. The optical absorption spectra of SB and PAZ-EP are shown in Fig. 6a. Taking into account the structure of the chromophoric units, such as multiple bonds ($-\text{C}=\text{C}-$, $-\text{CH}=\text{N}-$) and lone pairs of electrons (N, O), generating a delocalization along the polymer backbone, peak wavelengths tend to be shifted toward the long wavelength region as the conjugated system gets larger. The peaks of $\pi \rightarrow \pi^*$ electronic transition for the aromatic ring and azomethine ($-\text{CH}=\text{N}-$) group in SB and PAZ-EP were observed in the range of 270–290 nm and 273–314 nm; 290–331 nm and 314–348 nm, respectively. The characteristic absorption of $n \rightarrow \pi^*$ transitions for azomethine ($-\text{CH}=\text{N}-$) group of the synthesized SB and PAZ-EP were observed in the range of 332–355 nm and 348–366 nm, respectively. In comparison to the starting material (SB), it was possible to verify that the maximum peak at 330 nm for PAZ-EP was red-shifted with a broadened absorption.

The optical band gap values (E_g) were calculated using the formula of $E_g = 1242/\lambda_{\text{onset}}$ (Colladet et al. 2004) where λ_{onset} , the starting wavelength for the electronic transition (the onset wavelength) can be identified by intersection of two tangents on the absorption edges. Table 1 elucidated that the synthesized PAZ-EP had lower optical band gap than that of its Schiff base. E_g values calculated for the longer wavelength absorption maximum and absorption edge were found to be 3.77 and 3.38 eV for SB and PAZ-EP, respectively, which were close to the band gap values of organic semiconductors (Liu et al. 2009).

Figure 6b displayed the difference in visible color of PAZ-EP under room light and UV light. The pale yellow color of PAZ-EP turned into blue under UV-lamp. The reduction in the band gap after epoxidation resulted in easier electronic transition and made PAZ-EP more electro-conductive.

The photoluminescence spectrum of PAZ-EP in DMF solution is depicted in Fig. 7. The maxima of the photoluminescence emission peaks were located in the range of 439–456 nm with an emission of blue light and 538–556 nm with an emission of green light as a result of the excitation of PAZ-EP by UV and visible light, respectively. The emission intensity changes when the excitation wavelength changes. As depicted in Fig. 7a, when excited at 370 nm of UV light and 460 nm of blue light, PAZ-EP emitted blue and green fluorescence light at 455 and 553 nm with photoluminescence emission intensities of 400 and 221 a.u., respectively. This emission behavior has been reported in the literature for several polymeric systems. The origin of this phenomenon is considered to originate from the broad chain dispersity of the polymeric system studied (Qu and Shi 2004; Vaganova et al. 2000). In this study, the conjugated polymer was considered as bi-chromophoric system and each unit consisting of different conjugation behaved as a different chromophore group. As a result, the light was absorbed by a multitude of chromophores. In other words, the longer conjugated chains emitted the light with longer wavelength

Fig. 5 ^{13}C NMR spectrum of PAZ-EP**Fig. 6** **a** Absorption spectra of Schiff base (SB) and its polymer (PAZ-EP) in DMF, **b** the colors of PAZ-EP under sunlight and UV light

(470 nm), whereas the shorter conjugated chains emitted the light with shorter wavelength (360 nm), and thus the different fluorescence emission colors could be achieved by changing

the applied excitation wavelength (Qu and Shi 2004). Since DA and SB did not show any fluorescence property, imine bonds and epoxy connections along the polymer chain of PAZ-EP could be considered as bi-chromophoric units which emitted blue and green lights, respectively. PAZ-EP emitted blue and green colors when excited at 370 and 460 nm with their quantum yields of 2.4 and 1.1%, respectively.

Figure 7b shows the time-dependent (0–600 s) fluorescence measurements depending on excitation of 370 and 460 nm light. No obvious fluorescence changes were observed within 600 s under the same conditions, demonstrating that PAZ-EP was stable with respect to 370 and 460 nm of exciting light. It is noteworthy that the bicolor property made PAZ-EP be effective for the production of light emitting diodes.

Cyclic voltammograms (CVs) of SB and PAZ-EP in acetonitrile/DMSO mixture as the supporting electrolyte at room temperature under argon atmosphere were investigated to identify the highest occupied (E_{HOMO})–the lowest unoccupied (E_{LUMO}) energy levels and electrochemical band gaps (E'_g) using the oxidation (E_{ox}) and reduction (E_{red}) peak potentials depended on the following equations (Liu et al. 2001):

$$E_{\text{HOMO}} = -(4.39 + E_{\text{ox}}), \quad (1)$$

$$E_{\text{LUMO}} = -(4.39 + E_{\text{red}}), \quad (2)$$

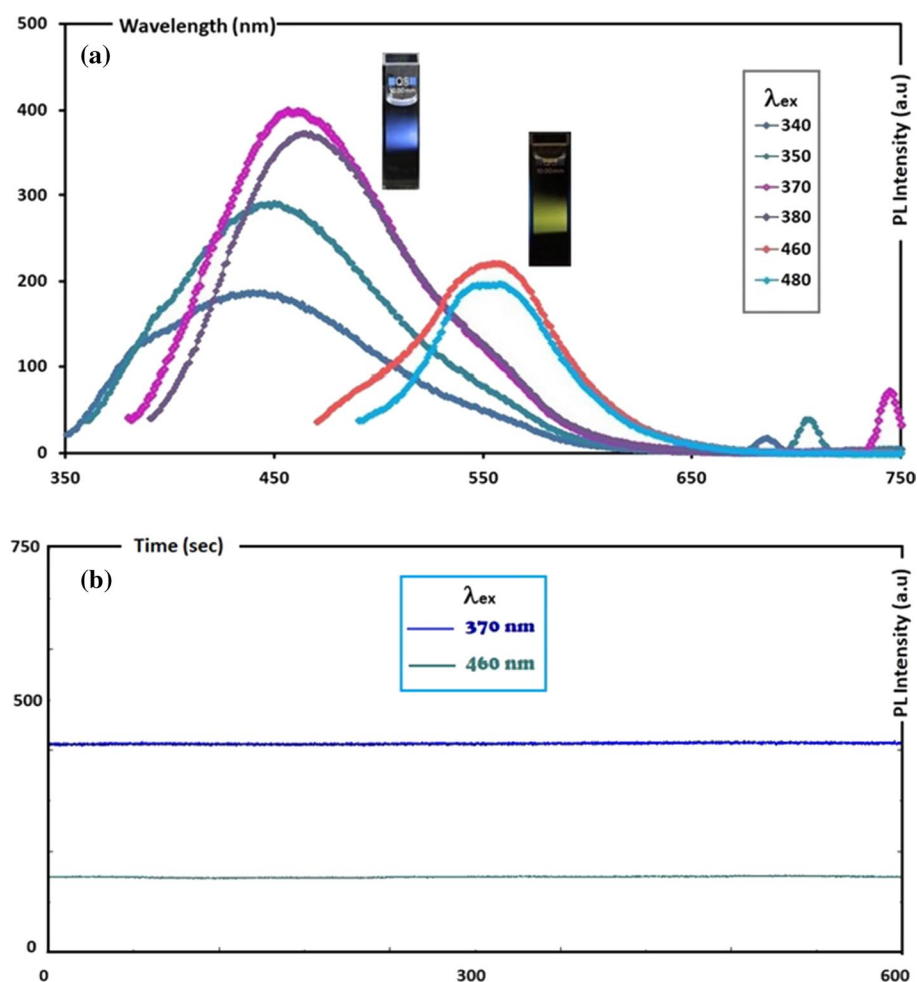
$$E'_g = E_{\text{LUMO}} - E_{\text{HOMO}}. \quad (3)$$

Table 1 Electronic and optical structure parameters of SB and PAZ-EP

	E_{ox} (eV)	E_{red} (eV)	HOMO (eV)	LUMO (eV)	λ_{onset} (nm)	E'_g (eV)	E_g (eV)
SB	1.512	-1.244	-5.90	-3.15	329	2.76	3.77
PAZ-EP	1.491	-1.195	-5.88	-3.19	368	2.69	3.38

$HOMO$ highest occupied molecular orbital, $LUMO$ lowest unoccupied molecular orbital, λ_{onset} absorbance wavelength, E'_g electrochemical band gap, E_g optical band gap

Fig. 7 **a** Photographs and the corresponding maximum emission spectra of PAZ-EP solution in DMF. Slit width: 5 nm and conc.: 10 mg L^{-1} in all measurements. Photographs were recorded in PL analysis cell. **b** Time-course fluorescence responses of PAZ-EP



An irreversible peak at both oxidation and reduction areas was observed for both SB and PAZ-EP. The reduction peak potentials of $-\text{HC}=\text{N}-$ via protonation of imine nitrogen were observed in the range of -1.19 and -1.24 V for SB and PAZ-EP. The peaks around 1.49 and 1.51 V were for the oxidation of hydroxyl groups (Bilici et al. 2010). According to Table 1, the values of (E'_g) and (E_g) values were found to be coherent.

Thermal properties

The thermal degradation (TGA-DTG) curves from ambient temperature to 1000 °C under nitrogen atmosphere are shown in Fig. 8. The values of the initial degradation temperature for T_{on} and the residual weight percent at 1000 °C (char %) are tabulated in Table 2. Based on Fig. 8 and Table 2, T_{on} and char % of PAZ-EP were lower than those of SB. This result indicated that PAZ-EP thermally decomposed more easily compared to SB since PAZ-EP owned easily cleavable ether linkages.

TG-DTG analyses clarified that thermal degradation of DA, SB and PAZ-EP took place in two stages as seen in Fig. 8. As indicated in Table 2, although (DA) and Schiff base had high thermal stability, the imine polymer (PAZ-EP) showed low thermal resistance, because T_{on} of DA and SB were obtained to be 301 and 281 °C, respectively, whereas PAZ-EP had 127 °C for initial degradation temperature. The temperatures corresponding to 20% of weight loss (T_{20}) were calculated as 321 , 316 and 151 °C, and the temperatures corresponding to 50% of weight loss (T_{50}) were figured out as 355 , 522 and 244 °C for DA, SB and PAZ-EP, respectively. SB decomposed in two steps starting from the temperature of 213 – 389 °C with 29.6% of weight loss then, 30% of weight loss was observed until 1000 °C. However, PAZ-EP degraded 40% of its initial weight in the temperature range of 39 – 216 °C. The second degradation in the range of 216 – 362 °C and the third degradation in the range of 366 – 1000 °C were analyzed with 36 and 12% of weight loss, respectively, until the end of the thermal study. The maximum rate of weight loss (T_{max}) values obtained from the derivative thermogravimetry (DTG) curves were found to be 342 °C; 303 and 438 °C; 159 , 245 and 442 °C,

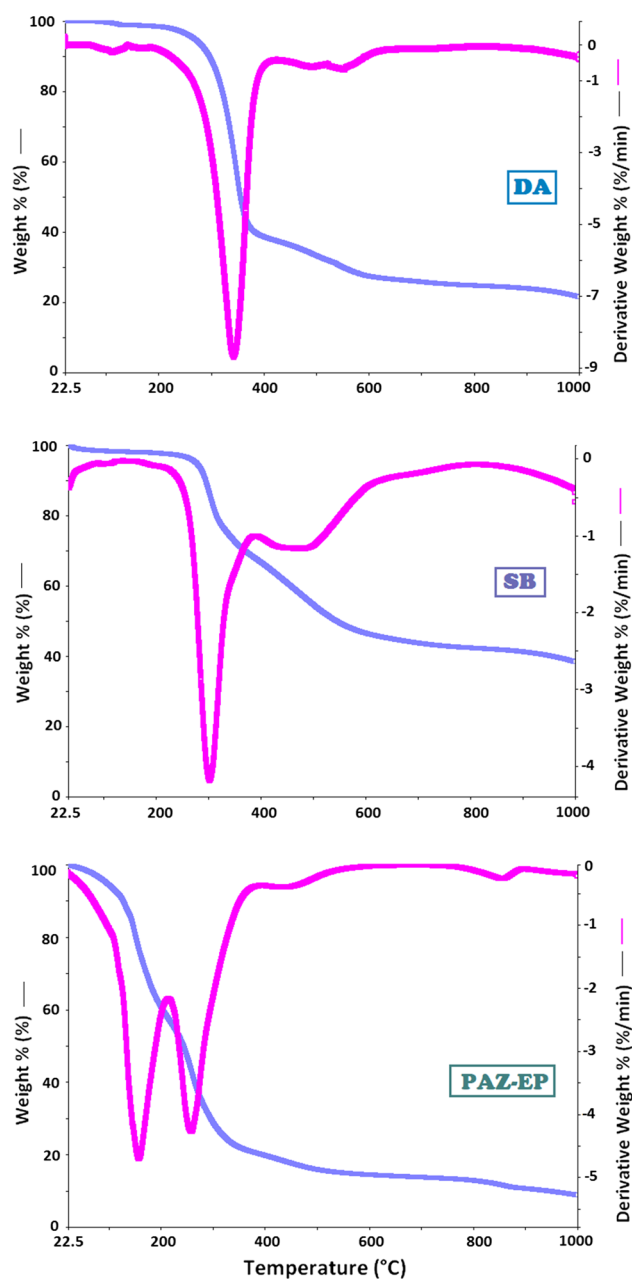


Fig. 8 TG/DTG profiles for (DA), (SB) and (PAZ-EP) at 10 °C heating rate in nitrogen atmosphere

indicating that the thermal degradation took place in one step, two steps and three steps for DA, SB and PAZ-EP, respectively. The weight loss curve of PAZ-EP with a T_{\max} value of 259 °C corresponded to ether linkage, and with a T_{\max} value of 442 °C, confirming that $-\text{N}=\text{CH}-$ group was breaking at this step (Saegusa et al. 1990; Grigoros and Antonoaia 2005).

The glass transition temperature (T_g) of PAZ-EP was studied by (DSC) and was found to be 113 °C. The melting point observed in DSC curve of SB at 109 °C was clearly

Table 2 Thermal degradation values of the synthesized compounds

	DA	SB	PAZ-EP
T_{on}	301	281	127
T_{max}	342	303, 438	158, 245, 442
20% weight loss	321	316	151
50% weight loss	355	522	244.8
char % at 1000 °C	22	38	9.2
DTA (endo/exo)	162/358	109/359	140/-
DSC [T_g (°C)/ ΔC_p (J g ⁻¹)]	-/-	-/-	113/1.208

T_{on} the onset temperature, T_{max} maximum weight loss temperature, T_g glass transition temperature, ΔC_p change of specific heat during glass transition

observed on DTA curve at the same temperature as an endothermic peak. Subsequently, the temperature at 359 °C corresponded to the degradation of imine bond seen as an exothermic peak on DTA curve.

In addition, the residual weight percent (char %) of DA, SB and PAZ-EP at 1000 °C were obtained as 22, 38 and 9.2%, respectively. In accordance with foregoing thermal analyses, it can be said that the synthesized imine polymer is not thermally stable with respect to its corresponding Schiff base.

Morphological properties

The morphology of PAZ-EP has been conducted by scanning electron microscopy (SEM). The preparation of PAZ-EP samples was performed using electro spinning system and vacuum spin coater, respectively. DMF was used to dissolve PAZ-EP with a solution concentration of 25 wt% in electro spinning. SEM views at different amplifications are shown in Figs. 9 and 10.

Then, SEM views of PAZ-EP demonstrated that particles were intertwined along the chain, as seen in Fig. 9. The cohesion property between the particles offered a stack of cottons, yielding a viscous yellow color form. The other process was to prepare a sample of PAZ-EP covered over a thin glass using a vacuum spin coater and let to dry in a vacuum oven at 50 °C for 2 days. Figure 10 denoted that the smooth surface of PAZ-EP with randomly aligned flat particles was morphologically different from the particles in Fig. 9. This difference is attributable to the processing variations in preparing the polymer samples for SEM analysis.

Conclusion

In a summary, PAZ-EP with epichlorohydrin was synthesized using Schiff base prepared by combining dialdehyde and diglycolamine agent. Methods of synthesis and detailed

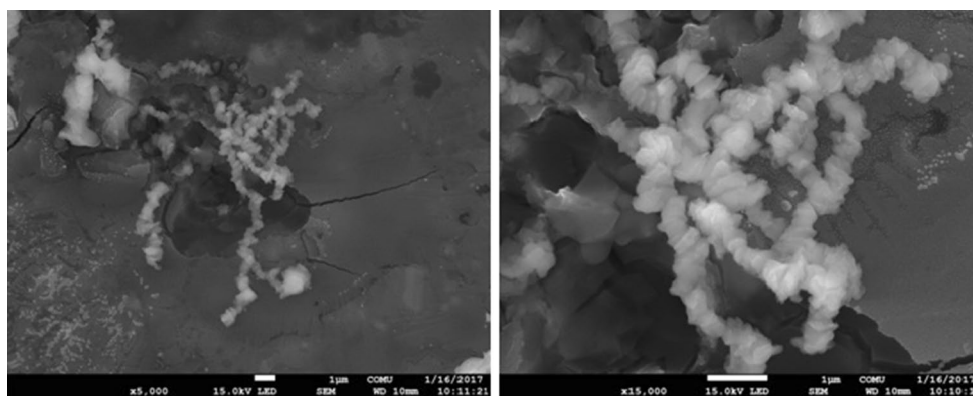


Fig. 9 SEM views of electro spinning results for PAZ-EP

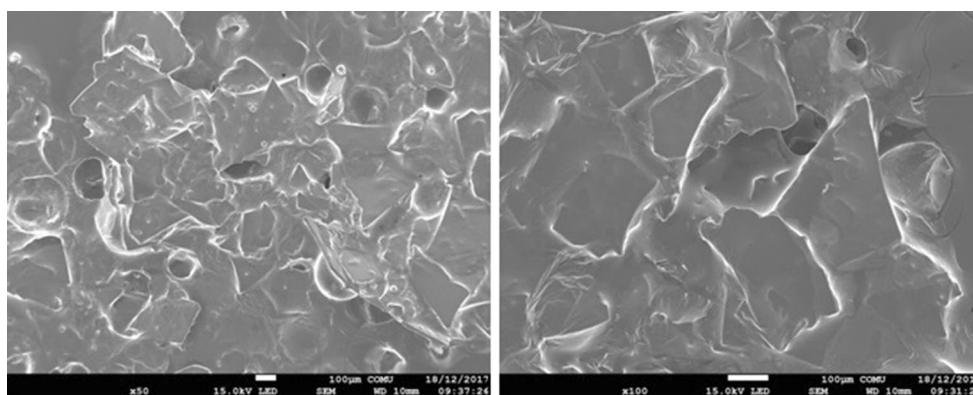


Fig. 10 SEM views of PAZ-EP prepared as a thin film

characterization of Schiff base and poly(azomethine-epoxy-ether) were presented. With a combined implementation of spectroscopic and electrochemical methods, the molecular structural details of poly(azomethine) containing ether linkages were studied in detail. The polymerization of azomethine-based compound (Schiff base) improved the thermal, photophysical and morphological properties. The incorporation of ether linkages and epoxy groups into the polymer backbone increased the solubility. Although the thermal stability of the polymer decreased, the optical and the electrochemical band gap values decreased via binding epoxies into the polymer chain. Based on the optical band gap value as in the case of semiconductors, PAZ-EP could be used in LED application (Kolcu and Kaya 2016). Fluorescent spectral studies indicated that PAZ-EP was a comprising model for a blue-light emitter. Depending on these attractive features, the synthesized PAZ-EP would improve photophysical properties with a lower band gap value than that of monomer. SEM views of electro spinning and spin-coating methods allowed obtaining different morphological properties. Thin film obtained by spin coating method showed flat surfaces

with epoxy side chains appeared to be smoother compared to the view obtained by electro spinning method. Film deposited by electro spinning method resulted in formation of granules intertwined with other granular particles. Increased solubility may also open the door to the processing potential of these materials for applications in polymer composites, protective coatings and for tuning the physical, thermal, and electrochemical properties of PAZ-EP. Curing process of PAZ-EP is under progress to enlighten its impacts on the thermal, optical and fluorescence properties of the polymer.

Acknowledgements The authors thank Çanakkale Onsekiz Mart University scientific research project commission for support with the Project number (Project no.: FBA-2017-1135).

References

- Abid KK, Al-barody SM (2014) Synthesis, characterization and liquid crystalline behaviour of some lanthanides complexes containing two azobenzene Schiff base. *Liq Cryst* 41:1303–1314. <https://doi.org/10.1080/02678292.2014.919670>

- Adams MC, Gannon JA (1986) Epoxy resins. In: Mark HF (ed) Encyclopedia of polymer science and engineering, 2nd edn. Wiley, New York, pp 322–382
- Barik S, Skene WG (2011) A fluorescent all-fluorene polyazomethine-towards soluble conjugated polymers exhibiting high fluorescence and electrochromic properties. *Polym Chem* 2:1091–1097. <https://doi.org/10.1039/c0py00394h>
- Bilici A, Kaya I, Yildirim M, Dogan F (2010) Enzymatic polymerization of hydroxy-functionalized carbazole monomer. *J Mol Catal B Enzym* 64:89–95. <https://doi.org/10.1016/j.molcatb.2010.02.007>
- Bourgeaux M, Skene WG (2007) A highly conjugated p- and n-type polythiophenoazomethine: synthesis, spectroscopic, and electrochemical investigation. *Macromolecules* 40:1792–1795. <https://doi.org/10.1021/ma070292p>
- Cerrada P, Oriol L, Pinol M, Serrano JL (1996) Alternative synthetic strategies for Schiff base derived liquid crystal polymers: a comparative study. *J Polym Sci Part A Polym Chem* 34:2603–2611. [https://doi.org/10.1002/\(sici\)1099-0518\(19960930\)34:13<2603::aid-pola6>3.0.CO;2-S](https://doi.org/10.1002/(sici)1099-0518(19960930)34:13<2603::aid-pola6>3.0.CO;2-S)
- Cervini R, Li XC, Spencer GWC, Holmes AB, Moratti SC, Friend RH (1997) Electrochemical and optical studies of PPV derivatives and poly(aromatic oxadiazoles). *Synth Met* 84:359–360
- Choi EJ, Ahn JC, Chien LC, Lee CK, Zin WC, Kim DC, Shin ST (2004) Main chain polymers containing banana-shaped mesogens: synthesis and mesomorphic properties. *Macromolecules* 37:71–78. <https://doi.org/10.1021/ma0348122>
- Colladet K, Nicolas M, Goris L, Lutsen L, Vanderzande D (2004) Low-band gap polymers for photovoltaic applications. *Thin Solid Films* 451:7–11. <https://doi.org/10.1016/j.tsf.2003.10.085>
- Dutta PK, Jain P, Sen P, Trivedi R, Sen PK, Dutta J (2003) Synthesis and characterization of a novel polyazomethine ether for NLO application. *Eur Polym J* 39:1007–1011. [https://doi.org/10.1016/S0014-3057\(02\)00328-2](https://doi.org/10.1016/S0014-3057(02)00328-2)
- Fukukawa K, Shibasaki Y, Ueda M (2004) Photosensitive poly(benzoxazole) via poly(*o*-hydroxy azomethine) II. Environmentally benign process in ethyl lactate. *Polym J* 36:489–494. <https://doi.org/10.1295/polymj.36.489>
- Grigoras M, Antonoia NC (2005) Synthesis and characterization of some carbazole-based imine polymers. *Eur Polym J* 41:1079–1089. <https://doi.org/10.1016/j.eurpolymj.2004.11.019>
- Grigoras M, Catanescu CO (2004) Imine oligomers and polymers. *J Macromol Sci Part C Polym Rev* 44:131–173. <https://doi.org/10.1081/mc-120034152>
- Grimm B, Krüger RP, Schrader S, Prescher D (2002) Molecular structure investigations on fluorine containing polyazomethines by means of the MALDI-TOF-MS technique. *J Fluor Chem* 113:85–91. [https://doi.org/10.1016/s0022-1139\(01\)00498-5](https://doi.org/10.1016/s0022-1139(01)00498-5)
- Gul A, Akhter Z, Siddiq M, Qureshi R, Bhatti AS (2014) Synthesis and physicochemical characterization of poly(azomethine)esters containing aliphatic/aromatic moieties: electrical studies complemented by DFT calculation. *J Appl Polym Sci* 13:40698–40706. <https://doi.org/10.1002/app.40698>
- Gutch PK, Banerjee S, Gupta DC, Jaiswal DK (2001) Poly-Schiff bases. V. Synthesis and characterization of novel soluble fluorine-containing polyether azomethines. *J Polym Sci Part A Polym Chem* 39:383–388. [https://doi.org/10.1002/1099-0518\(20010201\)39:383-388](https://doi.org/10.1002/1099-0518(20010201)39:383-388)
- Hussein MA, Abdel-Rahman MA, Asiri AM, Alamry KA, Aly KI (2012) Review on: liquid crystalline polyazomethines polymers. Basics, syntheses and characterization. *Des Monomers Polym* 15:431–463. <https://doi.org/10.1080/1385772x.2012.688325>
- Ishii J, Tanaka Y, Hasegawa M (2010) Film properties of polyazomethines (2). Poly(imide-azomethine)s derived from ester-containing dialdehydes, tetracarboxylic dianhydrides, and a fluorinated diamine. *High Perform Polym* 22:145–148. <https://doi.org/10.1177/0954008309349459>
- Işık D, Santato C, Satyananda B, Skene WG (2012) Charge-carrier transport in thin films of π -conjugated thiopheno-azomethines. *Org Electron* 13:3022–3031. <https://doi.org/10.1016/j.orgel.2012.08.018>
- Iwan A, Sek D (2008) Processible polyazomethines and polyketanils: from aerospace to light-emitting diodes and other advanced applications. *Prog Polym Sci* 33:289–345. <https://doi.org/10.1016/j.progpolymsci.2007.09.005>
- Kaya I, Culhaoglu S (2009) Syntheses, structures and properties of novel oligo(azomethine ether)s containing or not chlorine atoms in the main chain. *Polimery* 54:266–274 (WOS: 000264697600005)
- Kaya I, Doğan F, Gül M (2011) A new Schiff base epoxy oligomer resin: synthesis, characterization, and thermal decomposition kinetics. *J Appl Polym Sci* 121:3211–3222. <https://doi.org/10.1002/app.33843>
- Kaya İ, Ayten B, Şenol D (2018) Syntheses of poly(phenoxy-imine)s anchored with carboxyl group: characterization and photovoltaic studies. *Opt Mater* 78:421–431. <https://doi.org/10.1016/j.optmat.2018.02.057>
- Kobzar YL, Tkachenko IM, Bliznyuk VN, Shekera OV, Turiv TM, Soroka PV, Nazarenko VG, Shevchenko VV (2016) Synthesis and characterization of fluorinated poly(azomethine ether)s from new core-fluorinated azomethine-containing monomers. *Des Monomers Polym* 19:1–11. <https://doi.org/10.1080/1568551.2015.1092007>
- Kolcu F, Kaya I (2016) Synthesis and characterization of novel conjugated polyphenols of terephthaldehyde derived from symmetrical bis-azomethine groups in the polymer backbone via oxidative polycondensation. *J Macromol Sci A* 53:438–451. <https://doi.org/10.1080/10601325.2016.1176445>
- Koole M, Frisenda R, Petrus ML, Perrin ML, van der Zant HSJ, Dingemans TJ (2016) Charge transport through conjugated azomethine-based single molecules for optoelectronic applications. *Org Electron* 34:38–41. <https://doi.org/10.1016/j.orgel.2016.03.043>
- Krebs FC, Jørgensen M (2004) The effect of fluorination in semiconducting polymers of the polyphenyleneimine type. *Synth Met* 142:181–185. <https://doi.org/10.1016/j.synthmet.2003.08.015>
- Kumar S, Dhar DN, Saxena P (2009) Applications of metal complexes of Schiff bases—a review. *J Sci Ind Res* 68:181–187 (WOS: 000264035600001)
- Liu W, Lee SH, Yang SZ, Bian SP, Li L, Samuelson LA, Kumar J, Tripathy SK (2001) Biologically derived photoactive macromolecular azodyes. *J Macromol Sci Pure Appl Chem* 38:1355–1370. <https://doi.org/10.1081/ma-100108390>
- Liu P, Wu YL, Pan HL, Li YN, Gardner S, Ong BS, Zhu SP (2009) Novel high-performance liquid-crystalline organic semiconductors for thin-film transistors. *Chem Mater* 21:2727–2732. <https://doi.org/10.1021/cm900265q>
- Ma BB, Zhang H, Wang Y, Peng W, Wang MK, Shen Y (2015) Visualized acid–base discoloration and optoelectronic investigations of azines and azomethines having double 4-[*N,N*-di(4-methoxyphenyl)amino]phenyl terminals. *J Mater Chem C* 3:7748–7755. <https://doi.org/10.1039/c5tc00909j>
- Marin L, Cozan V, Bruma M, Grigoras VC (2006) Synthesis and thermal behaviour of new poly(azomethine-ether). *Eur Polym J* 42:1173–1182. <https://doi.org/10.1016/j.eurpolymj.2005.11.010>
- Marin L, Bejan A, Ailincăi D, Belei D (2017) Poly(azomethine-pheno-thiazine)s with efficient emission in solid state. *Eur Polymer J* 95:127–137. <https://doi.org/10.1016/j.eurpolymj.2017.08.006>
- Nitschke P, Jarzabek B, Wanic A, Domański M, Hajduk B, Janeczek H, Kaczmarczyk B, Musioł M, Kawalec M (2017) Effect of chemical structure and deposition method on optical properties of polyazomethines with alkyloxy side groups. *Synth Met* 232:171–180. <https://doi.org/10.1016/j.synthmet.2017.08.011>
- Niu HJ, Kang HQ, Cai JW, Wang C, Bai HD, Wang W (2011) Novel soluble polyazomethines with pendant carbazole and

- triphenylamine derivatives: preparation, characterization, and optical, electrochemical and electrochromic properties. *Polym Chem* 2:2804–2817. <https://doi.org/10.1039/c1py00237f>
- Park Y, Lee JH, Jung DH, Liu SH, Lin YH, Chen LY, Wud CC, Park J (2010) An aromatic imine group enhances the EL efficiency and carrier transport properties of highly efficient blue emitter for OLEDs. *J Mater Chem* 20:5930–5936. <https://doi.org/10.1039/c0jm00581a>
- Pron A, Rannou P (2002) Processible conjugated polymers: from organic semiconductors to organic metals and superconductors. *Prog Polym Sci* 27:135–190. [https://doi.org/10.1016/s0079-6700\(01\)00043-0](https://doi.org/10.1016/s0079-6700(01)00043-0)
- Qu L, Shi G (2004) Crystalline oligopyrene nanowires with multi-colored emission. *Chem Commun* 24:2800–2801. <https://doi.org/10.1039/b412638f>
- Ravikumar L, Kalaivani S, Vidhyadevi T, Murugasen A, Kirupha SD, Sivanesan S (2014) Synthesis, characterization and metal ion adsorption studies on novel aromatic poly(azomethine amide)s containing thiourea groups. *Open J Polym Chem* 4:1–11. <https://doi.org/10.4236/ojchem.2014.41001>
- Saegusa Y, Sekiba K, Nakamura S (1990) Synthesis and characterization of novel 1,3,4-oxadiazole-containing or 1,3,4-thiadiazole-containing wholly conjugated polyazomethines. *J Polym Sci Part A Polym Chem* 28:3647–3659. <https://doi.org/10.1002/pola.1990.080281311>
- Saegusa Y, Kuriki M, Nakamura S (1994) Preparation and characterization of fluorine-containing aromatic condensation polymers, 4. Preparation and characterization of fluorine-containing aromatic polyazomethines and copolyazomethines from perfluoroisopropylidene group-containing aromatic diamines and/or isopropylidene group-containing aromatic diamines and phthalaldehydes. *Macromol Chem Phys* 195:1877–1889. <https://doi.org/10.1002/macp.1994.021950535>
- Sek D, Iwan A, Jarzabek B, Kaczmarczyk B, Kasperczyk J, Mazurak Z, Domanski M, Karon M, Lapkowski M (2008) Hole transport triphenylamine–azomethine conjugated system: synthesis and optical, photoluminescence, and electrochemical properties. *Macromolecules* 41:6653–6663. <https://doi.org/10.1021/ma702637k>
- Shukla U, Rao KV, Rakshit AK (2003) Thermotropic liquid-crystalline polymers: synthesis, characterization, and properties of poly(azomethine esters). *J Appl Polym Sci* 88:153–160. <https://doi.org/10.1002/app.11618>
- Stefanache A, Balan M, Harabagiu V, Aubert PH, Guegan P, Farcas A (2014) Electro-optical properties of aromatic oligoazomethine/permethylated alpha-cyclodextrin main-chain polyrotaxanes. *Chem Phys Lett* 599:104–109. <https://doi.org/10.1016/j.cplett.2014.03.027>
- Vaganova E, Rozenberg M, Yitzchaik S (2000) Multicolor emission in poly(4-vinyl-pyridine). *Gel Chem Mater* 12:261–263. <https://doi.org/10.1021/cm990480x>
- Yeh LC, Huang TC, Lai FY, Lai HG, Lo AY, Hsu SC, Yang TI, Yeh JM (2016) Synthesis of electroactive polyazomethine and its application in electrochromic property and electrochemical sensor. *Surf Coat Technol* 303:154–161. <https://doi.org/10.1016/j.surfcoat.2016.03.094>
- Zhang WB, Wang C, Liu G, Wang J, Chen Y, Li RW (2014) Structural effect on the resistive switching behavior of triphenylamine-based poly(azomethine)s. *Chem Commun* 50:11496–11499. <https://doi.org/10.1039/c4cc05233a>